Wild or domestic? A 3D approach applied to crania to revisit the identification of mummified canids from ancient Egypt

C. Brassard, A. Evin, C. Ameen, S. Curth, M. Michaud, D. Tamagnini, K. Dobney, C. Guintard, S. Porcier, H. Jerbi

Wild or domestic? A 3D approach applied to crania to revisit the identification of mummified canids from ancient Egypt

Brassard C.[1,2,*], Evin A.[3], Ameen C.[4], Curth S.[5], Michaud M.[6], Tamagnini D.[7,8], Dobney K.[9,10,11,12], Guintard C.[13,14], Porcier S.[15], Jerbi H.[16]

[1] Fondation Fyssen, 194 rue de Rivoli, 75001 Paris, France

[2] MECADEV-UMR 7179, Muséum national d'Histoire naturelle, 75005 Paris, France

[3] ISEM, University of Montpellier, CNRS, EPHE, IRD, Montpellier, France, France

[4] Department of Archaeology, University of Exeter, Exeter EX4 4QE, UK

[5] Aquazoo Löbbecke Museum, Kaiserswerther Straße 380, 40474 Düsseldorf, Germany

[6] Department of African Zoology, Royal Museum for Central Africa, Tervuren, Belgium

[7] Department of Biology and Biotechnologies "Charles Darwin", University of Rome "La Sapienza", Rome, Italy

[8] Museum of Zoology, Sapienza Museum Centre, University of Rome "La Sapienza", Building, Viale dell'Universita 32, 00185 Rome, Italy

[9] Department of Archaeology, School of Philosophical and Historical Inquiry (SOPHI), Faculty of Arts and Social Sciences, University of Sydney, Sydney, Australia

[10] Department of Archaeology, Classics and Egyptology, University of Liverpool, University of Liverpool, 12-14 Abercromby Square Liverpool, L69 7WZ, UK

[11] Department of Archaeology, Univeristy of Aberdeen, St Mary's Building, Elphinstone Road, Aberdeen, AB24 3UF, UK

[12] Department of Archaeology, Simon Fraser University, Burnaby, B.C. V5A 1S6, Canada

[13] Laboratoire d'Anatomie comparée, Ecole Nationale Vétérinaire, de l'Agroalimentaire et de l'Alimentation, Nantes Atlantique – ONIRIS, Nantes Cedex 03, France.

[14] GEROM, UPRES EA 4658, LABCOM ANR NEXTBONE, Faculté de santé de l'Université d'Angers, France.

[15] ASM-UMR 5140, University of Paul-Valéry Montpellier 3, Labex ARCHIMEDE, France.

[16] Service d'anatomie, Ecole Nationale de Médecine Vétérinaire Sidi Thabet, CP2020, Tunisia.

[*] Corresponding author: co.brassard@gmail.com

Declaration of interest: none

Keywords: animal mummification; dog; ancient Egypt; geometric morphometrics; species determination

1. Abstract

Many of the million animals dedicated to the deities in Ancient Egypt were canids. In contrast to the rare textual sources, the abundance of skeletal remains offers the opportunity to address the question of rather wild or domestic canids were mummified. However, species identification from osteological material remains problematic because it relies on a simple qualitative appreciation or traditional biometric analyses with a low discriminatory power, paired with incomplete comparative reference samples. Here we propose a new method of identification based on cranial form using a 3D landmark based geometric morphometric (GMM) approach. We built predictive methods using a large reference sample of numeric models of crania of modern canids, including a variety of domestic breeds (N=69, 38 different breeds) as well as feral dogs (N=31), and all species of wild canids present in Africa or the Near East and likely to have been present in Ancient Egypt (N=157). We then applied these methods to a sample of ancient canid remains (N=41). We compared the effectiveness of multivariate discriminant analyses based on 3D GMM to that using traditional linear morphometric measurements (LMM) commonly taken in the field. GMM provided much better results than LMM, cross-validation percentages reaching over 97.5% when determining the domestic/wild status, and 96.4% when determining the species among a reduced sample of wild canids (versus 88.2% and 85.2 % in LMM). With 3D GMM we detected the presence of dogs, but also African golden wolves and, for the first time, Near Eastern gray wolves among the mummies.

2. Introduction

From the 1st millennium BC to the 4th century AD (Roman period), ancient Egyptians mummified millions of animals, including ibises, owls, snakes, crocodiles, fish, cats, and dogs (Murnane et al. 2000; Ikram 2013; Kitagawa 2016; Porcier et al. 2019). Some of these animals had a special status, which implied that their bodies were treated for post-mortem survival much like humans, yet most were classified as 'votive offerings' to gods and goddesses by Egyptologists. Among those, millions of mummified canids have been discovered throughout Egypt (Dunand et al. 2005, 2017; Ikram 2013; Kitagawa 2016). They were dedicated to the deities of Anubis and Wepwawet (depicted as a canid or a human with a canid head), which were associated with death and travel, recalling wild nocturnal canids (or feral dogs) that roamed human cemeteries (Brixhe 2019).

The precise identity of these two canid deities remains uncertain, however: i.e. whether each god depicts a wild canid or a domestic dog is still debated (Thiringer 2020). Numerous authors have identified Wepwawet as a wolf (*Canis lupus*), perhaps because it was sometimes depicted with a white or gray fur (Thiringer 2020), or because the ancient Greeks named Asyut (one of the most well documented dog necropolises) “Lycopolis” (city of wolf) in its honour. Others identify Wepwawet as a “jackal”, referring to depictions showing triangular pointed ears, long bodies and straight bushy tails. However, these representations may be somewhat misleading as the ancient Egyptians included symbolic codes in such depictions. For example, when represented, jackals are completely black (which corresponds to no known living species of jackal), likely because this color represented regeneration and was associated with Anubis (Schenkel 1963, 2007; Thiringer 2020). The distinction between wild species from art and text is therefore complex in ancient Egypt, where different perceptions of the taxonomic diversity associated with such symbolism likely existed. In all cases, however, a distinction between wild and domestic animals seemed important as they are frequently represented in opposing positions. For example, in the Middle Kingdom and Second Intermediate Period, the board game called ‘Hounds and Jackals’ was popular (Thiringer 2020).

This singular religious phenomenon, and the uncertainty surrounding the identity of the deities, thus raises a simple question: which canids were used for mummification? Whether wild canids or domestic dogs are represented in mummified offerings will provide insight into e.g. supply strategies (animals bred on purpose, captured from the natural environment or imported as exotics) and the relative importance of each in the religious practices of ancient Egyptians.

Unfortunately, texts describing practices surrounding canid mummification are scarce, being limited to rare and obscure epigraphic sources dating to the Greco-Roman period. For example, the *Jumilhac papyrus* (332 to 30 BC) testifies that three kinds of canids were protected, and that they were the subject of ambiguous considerations: a first type of tjesem dogs (tjesem is the ancient Egyptian name for "hunting dog", and it is used to designate a type of greyhound-like dogs) lived until an advanced age but suffered a rapid and premature death, while the second type did not get a proper burial, did not reach religious status, and had its body burned and its ba (i.e. soul, spirit) annihilated after death. A jackal (“ounech”) is also described, and its death was the object of celebrations (because it was considered as an enemy of Osiris) (Durisch Gauthier 2002; Bouvier-Closse 2003). Strabon, in his Geography,

indicates that "a cult and a gift of sacred food" existed for dogs at Cynopolis, which may have been generalized to all of Egypt (Yoyotte et al. 1997). Yoyotte and Charvet even suggested that pharaohs and some private persons had established agricultural domains whose income ensured the feeding of sacred animals and the maintenance of the priestly personnel assigned to their cults (Yoyotte et al. 1997, p. 152).

Given the scarcity of epigraphic documentation, and the diverse and ambiguous nature of artistic representations, it appears that the zooarchaeological record offers us an alternative way of addressing the question of what canids were mummified. Based on age-at-death data (most canid remains are from very young animals) and the frequent dental anomalies and pathologies observed on these remains, it has been proposed by both Egyptologists and archaeologists alike that most canid mummies were likely domestic dogs, deliberately bred for sacrifice by dedicated keepers (Dunand et al. 2005). Breeding dogs in captivity for sacrifice would have secured a steady and reliable supply of specimens, affording opportunities to satisfy high demand from pilgrims, and allowing such practices to operate at a large scale. However, wild canids were also occasionally collected (yet not clear whether after natural death or intentionally hunted), as attested by recovery of the bones of red or Ruppel's fox (*Vulpes vulpes* and *V. rueppellii*, respectively) and "jackal" from previous excavations (Kitagawa 2016; Brassard 2017; Dunand et al. 2017; Hartley 2017).

The identification of "jackal" in previous studies is somewhat problematic. A number of jackal species are native to Egypt and the surrounding region, including the golden wolf (*Canis lupaster*), the Ethiopian wolf (*Canis simensis*), the Side-Striped Jackal (*Lupulella adustus*), the Black-Backed Jackal (*Lupulella mesomelas*), and the Near-Eastern golden jackal (*C. aureus*). To date, conventional wisdom classified Egyptian jackals as a subspecies of the golden jackal (*Canis aureus;* Wilson and Reeder 2005, pp. 574–575). However, recent genetic studies have revealed that they most likely derive from another species altogether, one more closely related to the grey wolf. Whilst studies first suggested that African specimens belong to a cryptic subspecies of the grey wolf (*Canis lupus lupaster*; Rueness et al. 2011; Viranta et al. 2017), others posited they are a completely distinct species (the African golden wolf *Canis lupaster* also referred as *Canis anthus*), showing morphological convergence with Eurasian golden jackals (Koepfli et al. 2015). More recent whole genome analyses have suggested that it may well be a hybrid of the gray wolf and the 'Ethiopian wolf' (*Canis simensis;* Gopalakrishnan et al. 2018). Given that Egypt is at the crossroads between Africa and the Near East (where the golden jackal is present), it is possible that the Eurasian golden

jackal and the African golden wolf are both present in modern and ancient Egypt (Viranta et al. 2017). Moreover, other species of jackals are also present in other geographically close regions - for example the Side-Striped Jackal (*Lupulella adustus*), or the Black-Backed Jackal (*Lupulella mesomelas*) and should, therefore, be considered when assessing species identification from canid bones and mummies. Moreover, although there is no evidence that they have ever lived in Egypt, gray wolves from the Near or Middle East (corresponding to *C. l. pallipes* and *C. l. arabs* subspecies) may have been present among mummified canids, given the geographic proximity with Egypt and the ability of these animals to travel long distances (Castelló 2018) or be imported along well established trade routes. It is, therefore, important to revisit conventions in how we determine and categorize "dog/jackal" from zooarchaeological and mummified canids from Egypt, by including in our analyses comparative specimens of all the species likely to be found in Egypt.

Finally, the extent to which imported 'exotic' canids may have been used is still unknown. For example, though the African wild dog (*Lycaon pictus*) was unmistakably represented on carved monumental palettes during the Predynastic period (and only rarely during the Dynastic Period; Osborn and Osbornová 1998, p. 80), no osteological evidence supports its presence anywhere in the Egyptian territory (Brémont 2021). It is thus possible that it was imported from elsewhere in Africa. Indeed, animals were often represented in Egyptian art despite not being indigenous (e.g. fallow deer, baboon or elephant; Brémont 2021).

The current methods of determination of bones are problematic for several reasons. To date, the precise identification of canid species has relied on a macroscopic osteological description of bones, mainly skulls, mostly based on qualitative criteria (see Lortet and Gaillard 1903, 1907; Kitagawa 2016; Dunand et al. 2017; Hartley 2017). Measurements taken with calipers are also common, yet the exploration of the trends in these metrics are often limited to bivariate graphs or estimates of wither heights despite the availability of more advanced multivariate analytical methods (Brassard et al., 2021; Callou in Dunand et al., 2017). Moreover, all these previous studies unfortunately did not include all possible species of modern canids present in Africa or the Near East. Therefore, it is possible that some wild canids have remained undetected and that their prevalence in faunal assemblages of mummified canids could be more important than previously thought. The present study is the first to consider the full suite of wild and domestic canids likely present in the study region and will help establish a methodology for separating domestic dogs from wild canids.

Unfortunately, studies of mummified Egyptian canids have not included an examination of cranial size and shape using 3D geometric morphometrics (which consists in analyzing the 3D coordinates of anatomical landmarks on the external surface of the object in order to describe its size and shape). Yet, this approach allows for a more thorough description and statistical analyses of shape and has proven its ability to differentiate wild and domestic canids in other contexts (Drake et al. 2017; Ameen et al. 2019; Aurélie Manin 2020) or other taxonomically close species of mammals such as sheep and goats (Evin et al. 2022; Jeanjean et al. 2022). Advances in 3D data acquisition such as photogrammetry (which basic principle is to build a 3D model of the object from 2D photographs) allow easy and cheap data acquisition directly in the field or on museum collections (Evin et al. 2016; Fau et al. 2016). This technique is particularly promising for Egyptian zooarchaeological studies since transporting archaeological remains from the site or between administrative territories within Egypt is forbidden under cultural heritage laws, thus strongly limiting analytical techniques that cannot be undertaken in the field. Photogrammetry in Egyptian archaeological contexts has been limited to human mummies, artefacts, monuments and even sites (e.g. Lima et al. 2018; Prada and Wordsworth 2018; Abdelaziz and Elsayed 2019; Vasilyev et al. 2019). This is the first study to apply this technique to the examination of animal mummies.

In this study, we propose a novel 3D GMM based method for the identification of canid species from mummified remains, and above all the domestic versus wild status of these canids, based on cranial shape and size. We focus on complete crania (i.e. skull without the mandible) which are abundant and often very well preserved in dog catacombs or Museum collections. Moreover, their shape carries a strong phylogenetic signal (making it one of the elements for which species diagnosis is easiest). First, we assess the ability of cranial shape and size to distinguish between modern canids of known species, including a dataset of domestic dogs incorporating dogs of known breeds as well as feral specimens. We further sampled wild canid species present in Africa or the Near East and likely to have been present or imported into Ancient Egypt. We then applied predictive methods on a small sample of ancient canid remains from different dog catacombs found along the Nile valley and maintained in the collections in the Musée des Confluences in Lyon (France). We used multivariate statistics to optimize the exploitation of metric data, and compared the effectiveness of discriminant analyses based on 3D geometric morphometrics with that based on traditional morphometrics using linear measurements. To do so, we use morphometric analyses commonly used in evolutionary biology or zooarchaeology allowing us to assess

morphological variation and to discriminate between species (e.g. see Claude 2013; Fabre et al. 2014; Evin et al. 2020; Parés-Casanova et al. 2020; Jeanjean et al. 2022).

3. Materials

3.1. Modern reference sample

We investigated a total of 257 crania of modern canids collected from several institutions (the detailed information about the origin and constitution of this sample is provided in SI 1). Wild canids are represented by 157 specimens from 13 species of the genus *Canis*, *Lupulella*, *Lycaon*, *Otocyon* and *Vulpes* (Table 1). Modern domestic dogs are represented by 100 specimens from a minimum of 38 different breeds (some pure, and others being crossbreeds). Based on the assumption that ancient dogs may be similar in shape to medium-headed modern dogs rather than breeds with highly specialised morphologies we included in this sample 26 modern feral dogs from Tunisia, Egypt, and Turkey, as well as 5 modern beagles, whose skull shape is average among modern breeds (see Brassard et al. 2022). We also included long-headed dogs (i.e. dolichocephalic dogs, such as Greyhounds, Afghan hounds) and short-headed dogs (i.e. brachycephalic dogs, such as Bullmastiffs, Boxers) to account for a full range of domestic variability within our analyses. We estimated how long or short-headed the modern dogs are by calculating their cranial width (measure taken between the two zygomatic arches which corresponds to measurement CR30 in fig. 1) and length ratios (CR1), which corresponds to the cephalic index CI (Roberts et al. 2010). We arbitrary choose the cutoff values, to obtain balanced groups: dogs with a CI≥0.55 were considered brachycephalic, dogs with a CI≤0.50 were considered dolichocephalic and dogs with an intermediate CI were considered mesocephalic.

We only considered young, subadult, and adult specimens, with permanent teeth fully erupted (i.e. excluding the juveniles). This allows to limit ontogenetic variation since age is known to have a significant impact on skull morphology, which is all the more important in sexually immature canids (i.e. before 8-12 months, see Forbes-Harper et al. 2017; Brassard 2020). Specimens were divided into categories depending the degree of closure of the cranial sutures (Barone, 2010). We considered as subadults specimens with all the permanent teeth erupted but a suture between the basisphenoid and the basioccipital (*Synchondrosis sphenooccipitalis*) still open (between 6 and 8/10 months). Young specimens have the suture between the basisphenoid and presphenoid not completely closed (between 10 months and 1-2 years old) whereas it is completely closed in adult specimens (more than 1-2 years old). When the suture

between the basisphenoid and the presphenoide was not clearly visible, individuals were classified as 'young/adult?'. Subadults are sexually immature specimens, but we chose to keep them in the analyses as we want to propose a method with the widest possible range of application (in terms of age).

Our aim is not to assess morphological differences between age and sex categories. However, we were careful to provide a reference sample that was as comprehensive and balanced as possible. As such, subadults are always much rarer in proportion, but their presence will help identify subadults in the archaeological sample.

Table 1. Constitution of the modern sample in terms of species, breed, sex, and age at death. Sex information, when available, is provided in brackets as follows (female/male).

Species	Breed	N	By age			
			Subadults	Young	Adults	Young/adults?
Canis familiaris	Total including	100 (32,34)	10 (5,3)	31(8,15)	35(14,10)	24(2,5)
	Feral	31(13,15)	6(6,3)	13(4,7)	8(6,2)	4(0,3)
	beagles	5 (3,2)	0	1(1,0)	4(2,2)	0
	brachycephalic	28	1	11	16	0
	mesocephalic	32	2	9	13	8
	dolichocephalic	40	7	12	14	7
Canis lupus		16	3 (1,1)	11(2,3)	0	2
Canis lupaster		17	1 (0,0)	10(4,4)	4(2,1)	2(1,1)
Canis aureus		2	0	2(0,1)	0	0
Canis simensis		9	1 (0,0)	8(2,2)	0	0
Lycaon pictus		13	1 (1,0)	6(2,2)	4(0,1)	2(0,1)
Lupulella mesomelas		20	4 (1,2)	10(1,1)	1(0,0)	5(2,2)
Lupulella adustus		8	0	4(4,0)	1(1,0)	3 (0,3)
Vulpes vulpes		23	3 (1,1)	8(3,2)	3(1,1)	7(1,3)
Vulpes rueppellii		15	1 (0,0)	2(1,0)	12(2,5)	0
Vulpes pallida		10	1 (0,1)	2(0,2)	4(2,2)	3(0,1)
Vulpes chama		4	0	0	2(0,0)	2(0,2)
Vulpes zerda		13	1 (1,0)	3(1,1)	4(1,0)	5(0,1)
Otocyon megalotis		7	0	0	4 (1,3)	3(1,2)
Modern sample		**257**	**24 (10,7)**	**88 (28,30)**	**77 (26,24)**	**56 (7,21)**
Ancient mummies		**41**	**7**	**7(2,2)**	**14(1,0)**	**13 (1,1)**

3.2. Archaeological specimens

We analyzed 41 archaeological crania from ancient canid mummies collected in dog catacombs along the Nile Valley by Louis Lortet, Claude Gaillard, and Gaston Maspéro in the early 20th century. No precise date is available for these specimens, but some other dog mummies from the collection were radiocarbon dated, and the oldest date to the 30th Dynasty, around 360 BC (Richardin et al. 2017; Porcier et al. 2019). Geographic provenance is known only for 26 specimens; these are from Assiout, Assouan, Rôda, Saqqara, Tehneh, and Thebes

(Louqsor; see SI 1). Some identifications were proposed by previous authors (Lortet and Gaillard 1903, 1907), and are compared with the identification obtained in our study.

4. Methods

4.1. Data acquisition

4.1.1. 3D modeling

Scaled 3D models of the crania were obtained from different operators and by different methods, including photogrammetry, surface scanning (Einscan), and medical CT scan protocols (see SI 2 for details). The models were repaired, cleaned, simplified, and mirrored where needed using © 'Geomagic Wrap' (version 2013.0.1.1206) and 'MeshLab' (v2016.12; Cignoni et al. 2008).

4.1.2. 3D Geometric morphometrics (GMM)

Cranial shape was quantified from the 3D coordinates of landmarks placed by a single operator (first author CB) on the numerical models using the software 'IDAV Landmark', version 3.0.0.6 (©IDAV 2002-2005; Wiley et al. 2005). Forty-one unilateral landmarks were placed on the left side of the cranium (Table 1, Fig. 1) and were then mirrored for further visualizations, using function 'mirrorfill' from the package 'paleomorph' in R (R Core Team 2021). The resulting raw coordinates are available in the supplementary material (SI 3).

All following analyses were carried out in R, using mainly the packages 'Morpho' (Schlager 2017) and 'Geomorph' (Adams et al. 2016).

Mirrored landmarks coordinates were superimposed following a Generalized Procrustes Analysis (GPA) using function 'procSym' (Rohlf and Slice 1990; Goodall 1991; Mitteroecker and Gunz 2009; Dryden and Mardia 2016). During this procedure, the raw coordinates undergo translation, scaling and rotation to standardise the relative positioning of the specimens around their centroid to minimize the squared summed distances between corresponding landmarks (Rohlf and Slice 1990). Centroid size (CS) is the square root of the sum of squared distances of the landmarks from their centroid (Bookstein 1991) and measures the dispersion of the landmarks around the centroid. This can be used as a univariate summary of the overall size of the cranium. From this procedure we extracted the Procrustes coordinates and the log10-transformed centroid size, which are used to describe cranial shape and size, respectively. The new set of shape coordinates obtained from the GPA – namely

Procrustes coordinates – together represent the total amount of shape variation in the entire sample. When the analyses focussed only on certain specimens, new GPAs were conducted separately for each separate dataset (corresponding to further analyses, e.g. when considering all species or just some of them).

For visualizations of shape variation, the 3D surface scan of the cranium of a feral dog was warped onto the consensus shape of the GPA, and then deformed using thin-plate spline using the function 'tps3d' (Bookstein 1989).

Table 2. Definition of the landmarks used in this study following the Nomina Anatomica Veterinaria nomenclature (NAV, 2017).

landmark	Definition
1	Most rostral point of Os incisivum, between incisor teeth I1 in dorsal view (Prosthion)
2	Most rostral point of Os nasale, on the midline (Sutura internasalis)
3	Most rostral point on Sutura nasoincisiva
4	Point at the junction of Os incisivum, Os nasale and Maxilla
5	Most caudal point of Os nasale, on the midline (Sutura internasalis) and at the junction with Os temporale (Nasion)
6	Most medial point at the postorbital constriction on the curvature corresponding to Linea temporalis
7	Most lateral point of the Processus zygomaticus of Os frontale
8	Processus frontalis of Os zygomaticum
9	Most rostral point of the curvature of the lower edge of the Fossa sacci lacrimalis
10	Bregmatic fontanel, most medial point of the Sutura coronalis, on the midline (Bregma)
11	Most rostral and medial point on the Sutura lambdoidea on the midline
12	Most posterior end of Os occipitale (Inion, called Akrokranion by von den Driesch)
13	Point at the extreme convex curvature of the Tuberculum nuchale
14	Point at the extreme convex curvature of the Crista supramastoidea
15	Most medial point of the Tuberculum articulare of Pars squamosa of Os temporale
16	Most rostral point of Maxilla in ventral view, on the midline
17	Most caudal point of Os palatinum, on the midline
18	Caudally to molar tooth M2, in the recess medial to Tuber maxillae of Os Maxilla (on the Facies pterygopalatine)
19	Most caudal point of the Synchondrosis sphenooccipitalis, on the midline
20	Most lateral point of the Synchondrosis sphenooccipitalis, rostrally to the Bulla tympanica
21	Most ventral point of Foramen magnum of Os occipitale, on the midline (Basion)
22	Most caudal point of the Condylus occipitalis of Os occipitale in ventral view
23	Point on the Canalis n. hypoglossi of Os occipitale in ventral view
24	Ventral tip of the Bulla tympanica
25	Tip of Processus paracondylaris
26	Most dorsal and caudal point of the Foramen alare caudale
27	Most ventral and posterior point at the junction of the Processus zygomaticus of Os temporale and Os zygomaticum, on the Arcus zygomaticus
28	Most caudal point at the junction between Maxilla and Os zygomaticum, under Arcus zygomaticus and near the Tuber faciale
29	Most cranial point of the alveolus of the canine tooth, on lateral side
30	Most caudal point of the alveolus of the canine tooth, on lateral side
31	Most cranial point of the alveolus of the upper carnassial tooth P4, on lateral side
32	Point between the alveolus of P4 and M1 teeth, on lateral side
33	Point between the alveolus of M1 and M2 teeth, on lateral side
34	Most caudal point of Maxilla behind tooth M2
35	Most dorsal point of the Foramen infraorbitale
36	Most ventral point of the Foramen infraorbitale
37	Most caudal point of curvature at the junction of Maxilla and Arcus zygomaticus of Os zygomaticu on lateral side

38	Most ventral and caudal point of the Foramen rotundum and alare rostrale
39	Most rostral point of Meatus acusticus externus on lateral side
40	Most caudal point of Meatus acusticus externus on lateral side
41	Dorsal and caudal border of the Foramen magnum, on the midline (Opisthion)

285

286 *4.1.3. Linear morphometrics*

287 We chose 13 measurements following the nomenclature of Von den Driesch (1976) and
288 commonly used by archaeologists and Egyptologists (Table 3, Fig. 1). To obtain these
289 measurements, we calculated the Euclidean distance to the nearest 1 mm between
290 corresponding 3D landmark coordinates recorded during the GMM acquisition (Table 3). We
291 chose these measurements to represent the length, width and height of the cranium and avoid
292 measurements that may carry redundant information. To disentangle size and shape from the
293 LMM data (as done in GMM), we used the log-shape ratio method (Mosimann 1970).
294 Following this method, size was computed as the log10 of the geometric mean of all
295 measurements (i.e. isometric size), and shape as the log10 of each measurement divided by
296 the isometric size (shape ratios).

297 **Table 3.** Cranial measurements considered in this study following Von den Driesch (1976).

Measurement	Definition	Correspondance with landmarks
cr1	Prosthion-Akrokranion	1-12
cr8	Prosthion-Nasion	1-5
cr13	Median palatal length: staphylion prosthion	1-17
cr16	Length of the molar row (measured along the alveoli on the buccal side)	32-34
cr19	length of the carnassial alveolus	31-32
cr20	length of M1	
cr23	greatest mastoid breadth: greatest breadth of the occipital triangle: otion-otion	14-14’
cr28	height of the foramen magnum: basion-opisthion	21-41
cr30	zygomatic breadth: zygion - zygion	27-27’
cr32	Frontal breadth: Ectorbitale – Ectorbitale	7-48
cr34	greatest palatal breadth: measured across the outer borders of the alveoli	32-32’
cr36	Breadth at the canine alveoli	30-30’
cr40	height of the occipital triangle: akrokranion-basion	12-21

298

299

Fig. 1. Geometric and linear morphometric protocols: position of the landmarks captured on the cranium, and correspondence with the linear dimensions considered in our analyses according to Von den Driesch (1970). Landmark positions and linear measurement are described in Table 2 and 3, respectively. Anatomical features mentioned in Table 2 are indicated. A: lateral view; B: ventral view; C: dorsal view; D: caudal view; E: rostral view.

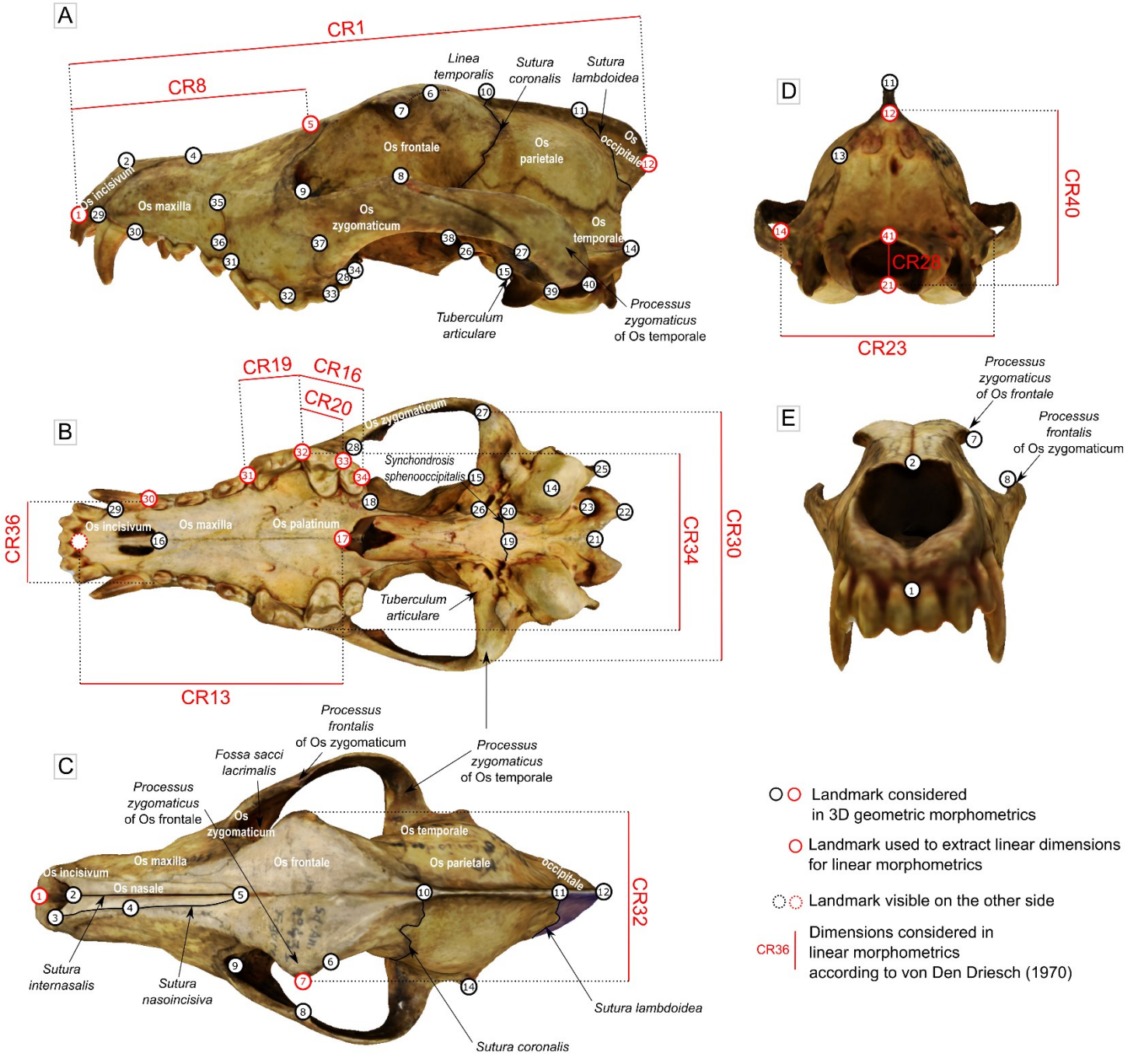

4.2. Inter species comparison

To refine our form descriptions and our interpretations, we performed analyses on (log10 transformed) centroid size and shape separately. We did not perform analyses on allometry-free shapes (allometry refers to size-related changes in shape; Klingenberg 2016).

Statistical analyses were performed following the same steps for 3D geometric (GMM) and linear morphometrics (LMM). First, differences between modern species were visualized using boxplots for size and principal component analysis (PCA) for shape (we used the function 'prcompfast' and a similar code as the source code of function 'procSym' to obtain the eigenvalues and scores). PCA reduces the dimensionality of shape data while preserving as much as possible of the information contained in the original data. Thus, the first factorial plane provides a representation of the overall variability in the dataset. The contribution of linear dimensions to the first axes of the PCA in LMM was visualized using barplots. In GMM, axes were interpreted based on visualizations and deformations from the consensus to the theoretical shapes at the minimum and maximum of the PC axes (which were computed using function 'restoreShapes'). The morphological differences between group means were visualized by deformations from the consensus to the mean shape of each species (SI 1). We explored differences in shape variability between dogs and wild canids through disparity tests (Foote 1997). Morphological disparity of each group was estimated as the Procrustes variance (i.e. the sum of the diagonal elements of the group covariance matrix divided by the number of observations in the group) using the residuals of a linear model fit (we used function 'morphol.disparity' with 999 permutations with the formula shape~1 to use the overall mean rather than group means; (Zelditch et al. 2012). We performed analyses by grouping together all the wild specimens of our study and then on all the species considered separately.

Differences in cranial size between species were tested using ANOVAs and post-hoc tests (using functions 'anova' and 'TukeyHSD'). Differences in cranial shape between wild versus domestic groups, and then between species, were tested using MANOVAs (function 'manova') followed by post-hoc tests (function 'pairwise.perm.manova' from package 'RVAideMemoire') on the scores of the non-zero PC components from the PCA in LMM. In GMM, we performed Procrustes ANOVA on Procrustes coordinates with a residual randomization permutation procedure (using function 'procD.lm' with 999 iterations and 'RPPP=TRUE'; (Goodall 1991; Collyer et al. 2015) and post-hoc comparisons (function 'parirwise' from package 'RRPP'). We also performed Canonical Variate Analysis (CVA)

with 10,000 permutations, following a separate GPA fit for each analysis in GMM (Campbell and Atchley 1981; Klingenberg and Monteiro 2005).

The discriminatory power of GMM and LMM was also assessed by linear discriminant analyses (LDA) paired with a leave-one-out cross-validation procedure to determine classification accuracy. Classification accuracy corresponds to the percentage of specimens correctly re-assigned to their own group. The leave-one-out procedure removes one specimen at a time, and predicts its classification into *a priori* defined reference groups using LDA function computed on all the remaining specimens (Evin et al. 2013). The procedure is repeated for each specimen in the sample, each in turn being treated as an unknown. This avoids predicting a specimen on the basis of a function computed on data that includes the specimen itself which would tend to spuriously inflate classification accuracy (Kovarovic et al. 2011).

A weakness of this method is that it is sensitive to the number of variables, sample size, and unbalanced design (see Mitteroecker and Bookstein 2011; Evin et al. 2013, 2015).The sensitivity to class size is particularly important considering that some species have a low occurrence in our primary dataset (e.g. *C. aureus* is only represented by two specimens, Table 1). Yet, large differences in sample size across groups may lead to the largest sample (i.e. dogs) dominating the pattern of variance covariance in the data, resulting in a higher chance of assigning ancient specimen to these larger groups leading to a possible misinterpretation of classification accuracy (Kovarovic et al. 2011; Evin et al. 2013). To solve the problem due to small sample size for some species, we first performed analyses to distinguish domestic dogs (N=100) and wild canids (N=157) by grouping together all the wild specimens of our sample. Then, we performed analyses on the wild candidate species that are closer to the archaeological specimens which were classified as wild by the previous LDA and after removing the species with the smallest sample sizes (e. g. *Canis aureus*).

To avoid the over-fitting of the data caused by the high number of variables and unbalanced design we performed analyses after dimensionality reduction and homogenization of group samples using the function ‘mevolCVP’ (from package ‘mevolCVP’). This function allows to determine the number of PCs needed in order to maximize the differences between groups. We replaced the original shape variables (Procrustes coordinates or shape ratios) with the scores of these first PCs (Baylac and Frieß 2005; Evin et al. 2013). In this procedure, perfectly balanced groups are obtained by a random selection (repeated 1000 times) of a number of specimens in the largest samples equal to the sample size of the smallest group. The outcomes

of this iterative resampling approach were summarized by the upper and lower 95th percentiles of cross-validation percentage (CVP).

4.3. Identification of archaeological specimens

After Procrustes superimposition the archaeological specimens were projected on the PCA with the modern specimens (using the same source code as in function 'PCA' from package 'FactoMineR'). The archaeological specimens were then assigned to the wild or domestic group through predictive LDA. We performed analyses after homogenization of groups by using the function 'pldam' from the package 'mevolCVP' following Evin et al. (2013). A specimen can be assigned to a group with higher or lower confidence depending on its relative distance to the group mean. The level of confidence is estimated by the posterior probabilities of classification as described previously. The highest posterior probability (which relates with the distance between the archaeological specimen and the mean of the groups) determines the classification of the specimen.

Finally, a PCA was performed on the wild specimens only in order to establish the list of the candidate species for further predictions of the wild canids among Egyptian mummies. We considered the wild species that are closest to the archaeological specimens on the first factorial plane of the PCA, and excluded the species with a low sample size (e.g. *Canis aureus*). We then performed a new predictive LDA to classify the wild specimens.

5. Results

5.1. Size differences between species

Differences in the mean centroid size exist between many species ($P_{AOV}<<0.001$, $R^2=0.80$ in both GMM; $P_{AOV}<<0.001$, $R^2=0.87$ and LMM; see supplementary material SI 4 for results of the pairwise comparisons). However, dogs exhibit a large amount of variation in size and strongly overlap with other canids for both GMM and LMM analyses (Fig. 2), making size alone an insufficient criterion for species identification or the separation of wild from domestic specimens.

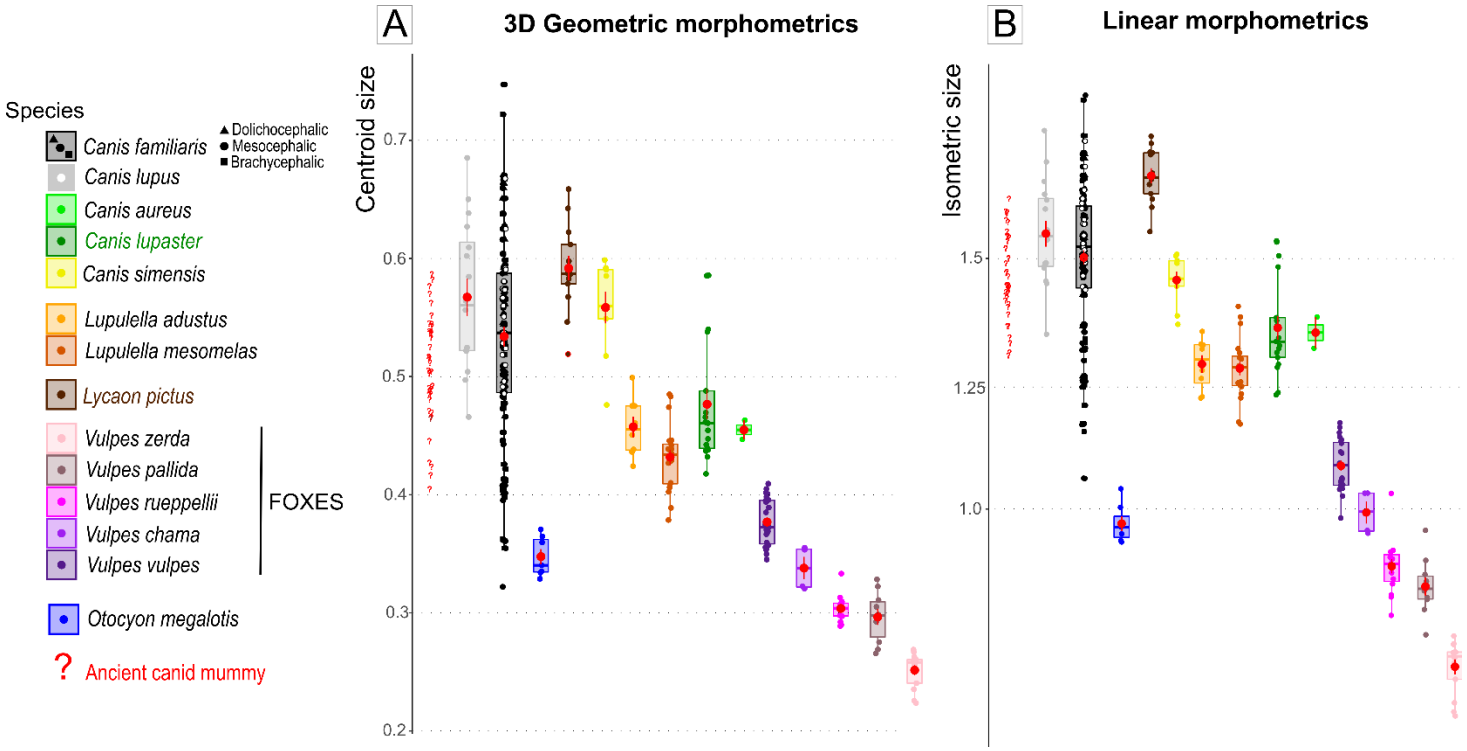

401 **Figure 2.** Visualization on boxplots of the variability in cranial size in ancient (N = 41) and
402 modern (N = 100 dogs and 157 wild specimens) canids according to GMM (A) and LMM (B)
403 analyses. Ancient dogs are represented by red question marks, and modern dogs are in black.
404 Modern wild species are indicated in different colors. Point shape indicates the morphotype of
405 modern dogs. See Table 1 and SI 2 for details about the sample. The red dots and red vertical
406 lines indicate the mean and standard deviation for each group.

407 ### 5.2. Shape differences between species

408 #### *5.2.1. Variability in dogs compared to wild African canids*

409 Dogs display as much intra-group variability in cranial shape as all the wild specimens in our
410 study when grouped together, as observable on the two first PCs of the PCAs (Fig. 3) and
411 demonstrated by the results of the disparity tests for both GMM and LMM analyses (GMM: P
412 = 0.042, Procrustes variance = 0.0061 in 100 dogs and 0.0052 in the 157 wild canids; LMM:
413 P = 0.4, Procrustes variance = 12.2 in dogs and 13.5 in wild canids). The GMM analyses even
414 tend to suggest a greater disparity in dogs compared to *C. lupus*, *C. lupaster* and *L. mesomelas*
415 (P < 0.003). Other comparisons are not significant when retaining a P value below 0.01 (see
416 SI 4 for details).

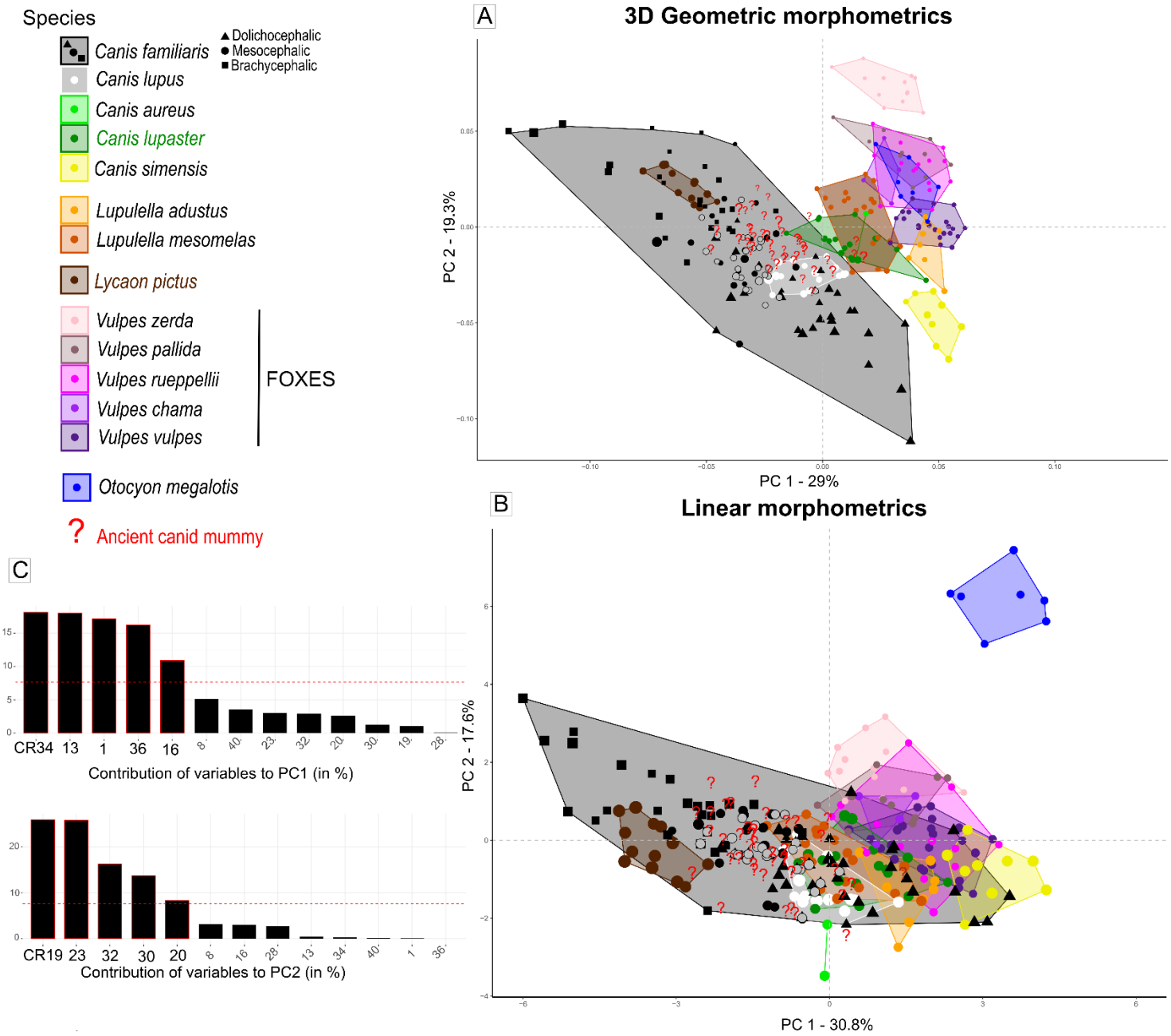

Figure 3. Visualization of the variability in cranial shape on the first factorial plane of the PCA in ancient (N = 41) and modern (N = 100 dogs and 157 wild specimens) canids according to GMM (A) and LMM (B) analyses. Icon size is proportional to the log10 of the centroid size. Ancient dogs are represented by red question marks, and modern dogs are in black. Modern wild species are indicated in different colors. Point shape indicates the morphotype of modern dogs. See Table 1 and SI 2 for details about the sample.

5.2.2. Differences in shape between wild and domestic groups

In both GMM and LMM analyses, highly significant differences are found in the mean cranial shape between domestic dogs and wild canids when grouped together (LMM: $P_{MANOVA} < 0.001$; GMM: $P_{Procrustes\ ANOVAs} < 0.001$, $R^2 = 0.16$).

Based on raw Procrustes data, the CVA shows that each specimen can be correctly classified between domestic and wild with an accuracy of 97.3% in GMM: only 5/100 dogs and 2/157 of the wild canids were not correctly assigned. Among the misidentified dogs, three are feral, one is a borzoi, and another is a dachshund. The two misidentified wild canids are Near Eastern wolves. When performing discriminant analyses on a balanced sample and a reduced dataset (we kept only the first 12 PCs, which account for only 78.4% of the total variance but are enough to discriminate species according to the results of the 'mevolCVP' function), we obtain similar discrimination power and percentages (accuracy of **97.5% [95% confidence interval: 97.46-97.59%]**). This confirms the robustness of the method.

LMM has less discriminatory power than GMM: the accuracy is lower, for both the CVA (89.1% 13/100 dogs and 15/157 of the wild canids were not correctly assigned) and the balanced LDA (performed on the first 8 PCs, which represents 93.7% of the total variance: CVP = **88.2% [88.09-88.30%]**).

5.2.3. Differences in shape between all species

When performing analyses with all species considered as separate groups, we found that, in GMM analyses, significant differences in the mean shape exist between all species except between *V. pallida* and *V. rueppellii*, between *C. lupaster* and *L. mesomelas*, and between *C. lupaster* and *C. lupus* ($P_{Procrustes\ ANOVAs} << 0.001$ see supplementary material SI 4 for results of the pairwise comparisons). In LMM, although significant differences in shape are globally found between species ($P_{MANOVA} < 0.001$, analyses performed on the 8th first PCs representing 93.7% of the total variance), the p-value in pairwise comparisons (when significant) is always close to 0.05, suggesting more subtle differences compared to GMM (see SI 4). Additionally, in LMM, the first factorial plane of the PCA is much less discriminating than for GMM (Fig. 3).

When considering species separately, the accuracy of the CVA is 94% in GMM, and 80.5% in LMM. However, these accuracies need to be explored further using balanced LDA on a larger and more robust sample. In GMM analyses, *L. adustus*, *L. pictus*, *C. simensis*, *V. vulpes*, *V. zerda* and *O. megalotis* have a classification accuracy of 100% (SI 4). In LMM analyses, only *L. pictus* and *O. megalotis* have a classification accuracy of 100%. In both GMM and LMM analyses, there is less accuracy in separating dogs and *C. lupus* (97% of dogs and 81% wolves are correctly assigned in GMM analyses, while the accuracy is of 91% for dogs and 50% for wolves in LMM analyses), between *C. lupus*, *C. lupaster* and *L. mesomelas*, and between *V.*

pallida and *V. rueppelli* (see SI 4 for details). *Vulpes chama* seems rather similar to *V. rueppellii* and *V. pallida*, while *C. aureus* is more similar to *C. lupaster* and *C. simensis*. Wolves show frequent misclassification (43.7% of wolves are misclassified), as well as *V. pallida*.

5.2.3. Differences in shape between C. lupus, C. lupaster and L. mesomelas

When considering only *C. lupus*, *C. lupaster* and *L. mesomelas* in our analyses, we evidence strong differences in the mean cranial shape between the three species in both GMM and LMM analyses (GMM: $P < 0.001$, $R^2 = 0.22$; LMM: $P < 0.002$). We also observe that *C. lupaster* (Procrustes variance = 0.0017) is less variable in shape than both *C. lupus* (Procrustes variance = 0.0024, P=0.009) and *L. mesomelas* (Procrustes variance = 0.0024, P = 0.008) in GMM analyses (results are not significant in LMM). We also obtain excellent classification rates in GMM analyses: more than 96% for the CVA on Procrustes data, which is confirmed by the high CVP in balanced LDA (**96.4 %** [96.3-96.5%]) performed on the first 7^{th} PCs (representing 63% of the total variance). The accuracy is lower in LMM analyses (81.1% for the CVA, **85.2 %** [84.9-85.6%] in the balanced LDA on the first 10 PCs).

5.3. Classification of ancient canid mummies

We observe that all ancient canids have cranial centroid sizes out of the range of *V. zerda*, *V. pallida*, *V. chama*, *V. rueppellii* and *O. megalotis* in the GMM analyses, and even *V. vulpes* in the LMM analyses (Figs 2 and 3, SI 5). Size thus helps with a preliminary exclusion of small canid species. This first sorting is even more efficient for the LMM method.

The preliminary CVA performed on raw Procrustes shape data and considering all species allowed to classify ancient canids into dogs (n=32), *C. lupaster* (n=5), and *C. lupus* (n=4; Table 4, SI 6). For the LMM analyses, the CVA classified canids into the same number of dogs (n=32), but the distribution between wild canids is different (3 *C. lupaster,* 3 *L. mesomelas,* 2 *C. lupus* and even 1 *L. pictus;* Table 4, SI 6), although the size of the specimen identified as a *L. pictus* is not compatible with this attribution.

The function 'pldam' identified 33 domestic dogs and 8 wild canids in both GMM and LMM analyses. However, class assignment is different between GMM and LMM analyses for four specimens (Fig. 4A, Table 4).

When these possible ancient wild canids are projected in the first factorial plane of the PCA performed on shape data (GMM) of the modern wild specimens they position close to *C.*

familiaris, *C. lupus*, *C. lupaster*, *C. aureus*, and *C. mesomelas* (Fig. 4B1,B3), which allows to refine the list of candidate species for further prediction analyses. When considering only *C. lupus*, *C. lupaster* and *L. mesomelas* in the balanced LDA, the function 'pldam' identifies 2 *C. lupus* and 6 *C. lupaster* among these canid mummies (Fig. 4C). For LMM analyses, there is more overlap between species in the PCA (Fig. B2, B4), and the function 'pldam' identifies 5 *C. lupaster* and 3 C. *lupus*. Only three specimens are attributed to the same wild species in GMM and LMM (2 *C. lupaster* and 1 C. lupus, Table 4).

Given the higher ability of GMM to distinguish between domestic and wild canids, and to distinguish between *C. lupus*, *C. lupaster* and *L. mesomelas*, we consider the attributions related to GMM analyses more reliable.

Accordingly, based on geometric morphometrics, we determine that the ancient canids present in our sample are 6 *C. lupaster*, 2 *C. lupus* and 33 *C. familiaris* (with a probability over 75% for all specimens; Fig. 4A, C). All these attributions are compatible with the range of centroid size between species, considering that some specimens are relatively young (Table 4, Fig. 2). One specimen identified as a *C. lupaster* has a rather large centroid (or isometric size) compared to modern golden wolves (CCEC. 51000004), all the more it is a young specimen.

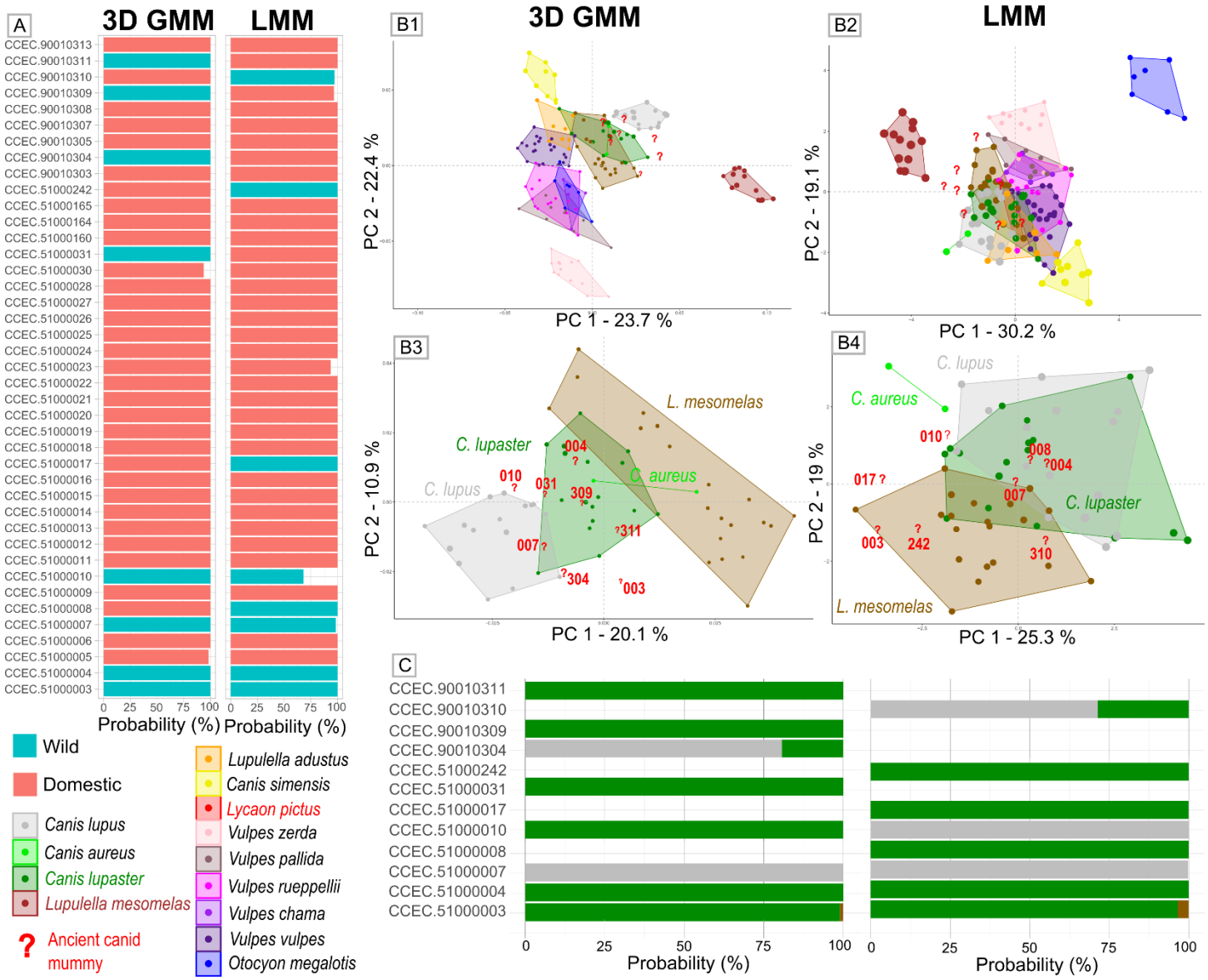

509 **Fig. 4.** Comparison of species predictions for archaeological dogs, in GMM versus LMM
510 analyses. A: Classification between wild and domestic: posterior probabilities of the balanced
511 LDA; B: Visualization of the variability in cranial shape on the first factorial plane of the
512 PCA in all ancient (N = 8) and modern (N = 157) wild specimens (B1, B2) or on the PCA
513 performed on the candidate species only (B3, B4) according to GMM (B1, B3) and LMM
514 (B2, B4) analyses. C: Classification of the wild canid mummies: posterior probabilities of the
515 balanced LDA.
516 In the PCAs, icon size is proportional to the log10 of the centroid size. Ancient dogs are
517 represented by red question marks, and modern wild species are indicated in different colors.
518 See Table 1 and SI 2 for details about the sample, and SI 6 for details about LDA attributions.
519
520
521

522

Table 4. Determination of wild canids among ancient specimens based on Geometric (GMM) and Linear morphometrics (LMM) and confrontation with data about size (Csize), age, previous determination and provenance. See SI 6 for detailed attributions and probabilities. See SI 7 for photographs of the archaeological specimen. CS: Centroid size; IS: isometric size; DOG: C. familiaris; WOLF: C. lupus; LUPA: *C. lupaster*; MESO: *L. mesomelas*. Previous determination: identification made by Louis Lortet and Claude Gaillard or written on the cranium. Refer to Figure 2 for the distribution of centroid and isometric sizes in modern species. CCEC.51000004 is rather large for a *C. lupaster*.

ID	Age	GMM 96.4%		LMM 87.3%		Previous determination	Geographic provenance
		LDA	CS	LDA	IS		
CCEC.51000003	Subadult-juvenile	LUPA	0.43	LUPA	1.31	*Canis aureus*	?
CCEC.51000004	young	LUPA	0.57	LUPA	1.55	*Canis doederleini* (Lortet & Gaillard, 1909: fig. 202-203)	Assouan
CCEC.51000007	adult	WOLF	0.55	WOLF	1.55	stray dog (Lortet & Gaillard, 1905: fig.4)	Roda
CCEC.51000008	young	dog	0.51	LUPA	1.45		Assouan
CCEC.51000010	Young /adult	LUPA	0.56	WOLF	1.58	*Canis sacer* (Lortet & Gaillard, 1909: fig. 199-200)	Louqsor
CCEC.51000017	Young/adult	dog	0.54	LUPA	1.59	Canis sp	Tehneh
CCEC.51000031	adult	LUPA	0.49	dog	1.45	Canis sp	?
CCEC.51000242	adult	dog	0.49	LUPA	1.47	Canis sp	?
CCEC.90010304	Young/adult?	WOLF	0.59	dog	1.59	Canis s	Tehneh
CCEC.90010309	subadult	LUPA	0.46	dog	1.37	Canis sp	Roda
CCEC.90010310	Young/adult?	dog	0.51	WOLF	1.45	Canis sp	Roda
CCEC.90010311	subadult	LUPA	0.49	dog	1.41	Canis sp	?

6. Discussion

6.1. Domestic versus wild and identification of wild canids

In this study, we demonstrated that 3D geometric morphometrics is a very powerful method for determining whether ancient mummified canids were domestic dogs or wild canids. In addition, we found it is much more accurate (with a degree of confidence of over 97%) than linear morphometrics (88%). We also obtained very satisfying results when determining species among wild canids for a subset of taxa that more closely resembled the ancient specimens (*C. lupaster*, *C. lupus*, *L. mesomelas*).

When considering the full suite of species likely present in the study region, the determination of species is more challenging, even when using 3D GMM (though results are much better than for LMM analyses). In particular, the distinction between *C. lupus*, *C. lupaster* and *C. mesomelas* or between *V. pallida* and *V. rueppellii* remains difficult. Several factors may come into play here. First, recent changes in the classification (and the ongoing evolution of taxonomic considerations, as raised in the introduction) made the constitution of the reference sample challenging. Our modern sample (even if representative of all relevant species)

contains few individuals in each group so may not fully represent the variability within the species, nor account for past variation not present in extant populations. Some species are particularly difficult to find in collections. For example, we had only one specimen of *Vulpes chama* (but as it is limited to the extreme south of Africa, it is unlikely to be found in ancient mummies) and only two *Canis aureus* (for most specimens identified as golden jackal in the collections, their location suggests that they were in fact *Canis lupaster*). Moreover, we did not find any specimen of bat-eared foxes (*Vulpes cana)* to include it in our study. The native range of this species along the Red Sea coastal mountains in eastern Egypt (as well as in the south of the Arabian peninsula and Iran; Castelló 2018, p. 207) makes it a more likely candidate for inclusion in mummified remains than foxes from more geographically distant areas (e.g. the cape fox *Vulpes chama*). Previous studies suggest that the skull of *V. cana* can be easily distinguished from that of *V. rueppellii* (with which it is sympatric throughout its known African range) by its "smaller size, sharply pointed and relatively long snout" (Saleh et al. 2018, p. 18). It is also larger than *V. zerda* (Castelló 2018, p. 207). Previous studies based on linear morphometrics have shown clear differences between Eurasian golden jackals and African golden wolves, yet morphometric comparisons of cranial shape between these species are scarce. Further research is, therefore, needed before a full evaluation of their presence or absence as mummified remains can be made.

Second, some wild canid species are very similar in shape (see SI 1) due to strong morphological convergence, with specimens displaying remarkably similar phenotypes to the point of being mistaken by trained biologists. This may explain our difficulties in distinguishing between *C. lupus*, *C. lupaster* and *C. mesomelas* or between *V. pallida* and *V. rueppelli*. Moreover, it is not impossible that some modern specimens from the collections were originally misidentified, thus biasing the results of our predictive models. In our study, *C. lupaster* occupies an intermediate and overlapping morphospace position (Figs 2, 4B) between jackal-like forms and wolf-like forms, as found in previous studies (Machado and Teta 2020). These morphological similarities are in line with previous GMM studies that showed important variation within *Canis lupaster*, with some subspecies showing morphological convergence with other species (e.g. between *C. l. soudanicus* and *L. adusta*, or between *C. l. bea*, *L. mesomeleas* and *C. aureus*). A robust species determination can be postulated by considering the species' current African or near Eastern distribution (when not sympatric), but this cannot be definitive since it presumes that species ranges and distributions have not changed over time.

A third significant challenge hinges on the fact that sympatric members of the genus *Canis* can readily hybridize in the wild, and that some of those hybrids are viable and able to form taxonomic complexes that are "ecologically and morphologically distinct from their parent species" (Gopalakrishnan et al. 2018; Machado and Teta 2020). Past hybridization and admixture between domestic and wild canids has been proven, for example, between dogs and African golden wolf (Bahlk 2015; Mallil et al. 2020), golden jackals (Galov et al. 2015) or Iranian wolves (*C. lupus pallipes;* Khosravi et al. 2013). The roaming of feral dogs in ancient Egypt may have promoted this hybridization and could explain why some ancient specimens were more difficult to classify between domestic and wild types. Other studies have identified gene flow between Eurasian golden jackals from Israel and gray wolves, dogs, and the African golden wolf (Koepfli et al. 2015), and between the Ethiopian wolf (*C. simensis*) and the African golden wolf (Bahlk 2015). Some studies have even suggested that the African golden wolf may originate from the hybridization between gray and Ethiopian wolves (Gopalakrishnan et al. 2018).

None of these limitations regarding species identification necessarily represent a major obstacle for studies of mummified canid remains. On the one hand ancient Egyptians had a different concept of species classification than we do (Charron 2002). On the other, what also interests us is to obtain information on the supply strategies/sourcing of the animals and related insights into mummification practices in conjunction with religious beliefs. Therefore, the most important classification to be made is between domestic and wild, and the method we outline here is excellent at doing so.

6.2. Statistical bias

By considering large groups (i.e. domestic/wild and *C. lupus*/*C. lupaster*/*L. mesomelas*) in our analyses and performing analyses on balanced samples and on the most discriminant PCs, we reduced the number of predictors to below that of the number of individuals of the smallest group and we ensured a satisfying number of specimens to define the reference groups in balanced analyses (n=100 in analyses separating between domestic and wild, i.e. the number of dogs; and n=16 in analyses on the candidate species only, i.e. number of *C. lupus*, Table 1). We can thus consider that our results are robust (Kovarovic et al. 2011). This is all the more important in the case of dogs, considering their tremendous diversity in cranial shape (which is as important as all wild species combined. This result is in line with those of Drake and Klingenberg (2010) who found that "the amount of shape variation among modern domestic dogs [much of which being the result of 200 years of intensive breeding] far exceeds that in

613 modern wild species, and it is comparable to the disparity throughout the Carnivora"; Figs 2
614 and 3). However, a larger sample for each wild species would be needed to provide a more
615 accurate estimate of the precision of our method for wild canids.

616 Additionally, the metadata on the modern sample did not allow us to account for sex or age
617 differences. Due to the determinant role played by sexual dimorphism and ontogeny in cranial
618 shape (Younes and Fouad 2016; Brassard 2020; Machado and Teta 2020), more modern
619 specimens of known sex and age for each species are needed to build more accurate predictive
620 models for example to apply on different age categories of archaeological remains.

621 **6.3. Geometric versus linear morphometrics applied to archaeological remains**

622 To date, Egyptologists have identified cranial remains based on macroscopic criteria (e.g. the
623 relative size of the carnassial, which is unfortunately not always still present in the alveola, or
624 tympanic bubble). Metrics appears useful to classify mummified remains more objectively
625 and are necessary for the examination of large datasets. Linear morphometrics are not
626 sufficient, however, and (as we demonstrate here) 3D geometric methods undoubtedly brings
627 an additional refinement for the identification of species and for estimating wild/domestic
628 ratios in large assemblages.

629 Among the isolated crania of canid mummies from the Musée des Confluences, we identified
630 mainly dogs, but also eight wild canids, belonging to either Near Easter grey wolves or
631 African golden wolves. Ancient DNA analyses would be necessary, however, to confirm our
632 final determinations and thus assess the reliability of the 3D GMM method when applied to
633 ancient remains.

634 One of the mummified canids identified as an African golden wolf (*C. lupaster)* is from Roda,
635 others are from Assouan and Louqsor (Table 6). Those identified as gray wolves (*C. lupus*)
636 are from Roda and Tehneh. Unfortunately, due to the inconsistent recovery and curation
637 practises of the early 20th century, the specimens hosted in many museum collections are
638 rarely properly contextualized (the provenance is not even always known), limiting our
639 interpretations. It will thus be crucial to study specimens from the field to go beyond the
640 simple determination and description, and provide conclusions on the sourcing of the animals.
641 To our knowledge, this is the first study to consider the presence of Near Eastern wolves
642 among canid mummies. It will be necessary to enrich both our modern and archaeological
643 databases prior to questioning deeper the use of this species for mummification.

Although showing traits qualitatively indicating its identification as a dog (see SI 7), the cranium of one mummy was clearly attributed to *C. lupaster* (with a probability over 90%, CCEC.510000031, see SI 6). Surprisingly, it shows an advanced degree of dental wear and many dental abnormalities. In particular, it shows signs of advanced periodontitis, with osteolysis at the root of the molars and oronasal fistula (SI 8). Although this is most often observed in domestic dogs or captive animals, Bertè (2017) has described similar traits in a specimen of *C. lupaster* caught from the wild at the oasis of Giarabub (specimen MSNG 26228, collected in 1926-1927 by C. Confalonieri; Bertè 2017). The frontal bone of this canid is deformed on both sides and its zygomatic process is very developed (somewhat abnormally), which may bias our determination. This individual could also be a hybrid, or an animal taken from the wild and then bred in captivity. Our identification for this specimen is thus to be taken with caution pending further analysis of other available bones, such as the mandible.

Although 3D GMM is efficient for species determination, this method should be seen as is complementary to the qualitative/morphoscopic approach, since it only partially captures shape compared to the human eye. Our own results may have been better had we used sliding semi-landmarks on curves and surface landmarks (i.e. landmarks placed on the whole external surface of the skull). However, this would have allowed us to capture only the skulls with an intact surface, thus reducing our sample size. We instead considered only a limited number of anatomical landmarks to be able to include also crania with a slightly damaged surface (including crania which retained residues of mummified tissue; see example in SI 7).

Due to the special nature of the materials under study, we were fortunate enough to have access to significant numbers of complete crania, an uncommon feature of most zooarchaeological collections. Three-dimensional GMM methods can also be applied to fragmented remains more efficiently than linear morphometrics, and we could easily adapt the landmarking protocol to different fragmentation patterns to include more specimens in the analyses, using a subset of the landmarks considered in this paper (for example see Brassard et al. 2022). Moreover, we only analyzed isolated crania, but 3D models could be obtained from medical scanners to access the data without the need to unwrap the mummy.

7. Conclusions and future perspectives

Geometric morphometrics provide a more efficient way of identifying crania in mummified canids from Ancient Egypt compared to traditional linear morphometrics. Based on a sample

of 100 modern dogs and 157 modern specimens of 13 wild species from Africa and the Near or Middle East, this study revealed clear differences between modern domestic dogs and wild canids, based on the shape of their cranium. Results revealed that the majority of mummified canids included in this dataset were the remains of domestic dogs. However, the reference sample we used needs to be further expanded to ensure it better represents the full diversity of shape in wild canids. Ancient DNA analyses could be deployed on the same specimens to cross-validate the results with the predictions based on 3D GMM in order to assess the reliability of our method. Once confirmed, the next step would be to apply this method to specimens photographed *in situ* in dog catacombs to further explore the diversity in mummified canids in contextualized sites. Moreover, once wild specimens are identified and removed from the analyses, it will be possible to further explore the diversity of ancient dogs to explore whether, for example, some particular morphologies were favoured over others, or if assumptions can be made on their living condition (feral, captivity), thus opening new perspectives pertaining to the source of canids used for mummification.

Acknowledgements

We thank Museums for providing access to their collections, in particular Didier Berthet and the Centre Louis Lortet – Musée des Confluences (Lyon, France), Géraldine Véron and the Muséum national d'Histoire naturelle (Paris, France), Stefan Hertwig and the Naturhistorische Museum Bern (Bern, Switzerland), Daniela Schweizer and the Vetsuisse Faculty of the University of Bern (Switzerland), Christiane Funk and the Museum für Naturkunde - Leibniz Institute for Evolution and Biodiversity Science (Berlin, Germany), Emmanuel Gilissen and the RMCA Museum, and the Harvard Museum of Comparative Zoology. We thank Anne-Claire Fabre for providing 3D models of specimens and people who provided access to surface or CT-scan facilities (including Anthony Herrel and the University Hospital in Jena, Germany) or financial support for some of the 3D acquisitions (including Greger Larson). We are very grateful to Anthony Herrel for proofreading the first version of this manuscript.

Author Declarations

Funding. The research leading to these results received funding from the Fyssen foundation, the 'investissement d'avenir' project Labex BCDiv (10-LABX-003) and the European Research Council.

Competing Interests. The authors have no competing interests to declare that are relevant to the content of this article.

Ethics approval. Not applicable

Consent to participate. Not applicable

Consent for publication. Not applicable

Data availability. All data generated or analyzed during this study are included in this published article (and its supplementary information files). All three-dimensional models of the crania are available in SI 9. Detailed information about the sample and methods are provided in SI 2. Raw 3D coordinates of the landmarks considered in GMM analyses are in SI 3.

Code availability. The R code is available from C.B. on request.

Authors' contributions. C.B. conceptualized the project, set up the study, acquired data, performed the statistical analyses and wrote the first draft of the manuscript. A.E., A.C., S.C., M.M. and D. T. provided 3D models for shape analyses. H.J. and C.G. collected part of the material and gave access to it. A.E. gave advise for the statistical analyses and was a major contribution in analyzing the data. H.J. is responsible for project administration and supervision. The manuscript was edited by C.B., A.E., A.C., S.C., M.M., D.T., K.D. and S.P. All authors gave final approval for publication and agreed to be held accountable for the work performed therein.

References

Abdelaziz M, Elsayed M (2019) Underwater photogrammetry digital surface model (DSM) of the submerged site of the ancient lighthouse near Qaitbay fort in Alexandria, Egypt. Int Arch Photogramm Remote Sens Spat Inf Sci. https://doi.org/10.5194/ISPRS-ARCHIVES-XLII-2-W10-1-2019

Adams DC, Collyer M, Kaliontzopoulou A, Sherratt E (2016) geomorph: Software for geometric morphometric analyses

Ameen C, Feuerborn TR, Brown SK, et al (2019) Specialized sledge dogs accompanied Inuit dispersal across the North American Arctic. Proc R Soc B Biol Sci 286:20191929. https://doi.org/10.1098/rspb.2019.1929

Aurélie Manin AE (2020) Canis spp. identification in central Mexico and its archaeological implications

737 Bahlk SH (2015) Can hybridization be detected between African wolves and sympatric
738 canids?

739 Barone R (2010) Anatomie comparée des mammifères domestiques : Tome 1, Ostéologie, 5e
740 édition. Vigot, Paris

741 Baylac M, Frieß M (2005) Fourier Descriptors, Procrustes Superimposition, and Data
742 Dimensionality: An Example of Cranial Shape Analysis in Modern Human
743 Populations. In: Slice DE (ed) Modern Morphometrics in Physical Anthropology.
744 Springer US, Boston, MA, pp 145–165

745 Bertè DF (2017) Remarks on the skull morphology of Canis lupaster Hemprich and
746 Herenberg, 1832 from the collection of the Natural History Museum "G. Doria" of
747 Genoa, Italy. Nat Hist Sci 4:19–29. https://doi.org/10.4081/nhs.2017.318

748 Bookstein FL (1991) Morphometric Tools for Landmark Data. Geometry and Biology,
749 Cambridge University Press

750 Bookstein FL (1989) Principal warps: thin-plate splines and the decomposition of
751 deformations. IEEE Trans Pattern Anal Mach Intell 11:567–585.
752 https://doi.org/10.1109/34.24792

753 Bouvier-Closse K (2003) Les noms propres de chiens, chevaux et chats de l'Égypte ancienne.
754 Le rôle et le sens du nom personnel attribué à l'animal. Anthropozoologica 37:11–38

755 Brassard C (2017) Le chien en Egypte ancienne : approche archéozoologique et apports de la
756 craniologie. Application a une série de chiens momifiés (El-Deir) et comparaison avec
757 des chiens actuels et anciens (Kerma). Thèse d'exercice, Vetagro Sup campus
758 vétérinaire de Lyon, Université Claude-Bernard Lyon 1

759 Brassard C (2020) Morphological variability in dogs and red foxes from the first European
760 agricultural societies: a morpho-functional approach based on the mandible.
761 Unpublished PhD thesis, Muséum national d'Histoire naturelle

762 Brassard C, Bălăşescu A, Arbogast R-M, et al (2022) Unexpected morphological diversity in
763 ancient dogs compared to modern relatives. Proc R Soc B Biol Sci 289:20220147.
764 https://doi.org/10.1098/rspb.2022.0147

765 Brassard C, Callou C, Porcier S (2021) To Be or Not to Be a Dog Mummy: How a Metric
766 Study of the Skull Can Inform on Selection Practices Pertaining to Canid
767 Mummification in Ancient Egypt. In: The Ancient Egyptians & the Natural World.
768 Sidestone Press, Cairo, Egypt

769 Brémont A (2021) Newcomers in the Bestiary. A Review of the Presence of Lycaon pictus in
770 Late Predynastic and Early Dynastic Environment and Iconography

771 Brixhe J (2019) Le chien dans l'Egypte ancienne: les origines. Club Royal Belge du Lévrier.

772 Campbell NA, Atchley WR (1981) The geometry of canonical variate analysis. Syst Zool
773 30:268–280. https://doi.org/10.2307/2413249

774 Castelló JR (2018) Canids of the World: Wolves, Wild Dogs, Foxes, Jackals, Coyotes, and
775 Their Relatives. Princeton University Press

776 Charron A (2002) Taxonomie des espèces animales dans l'Egypte gréco-romaine. Taxon
777 Espèces Anim Dans Egypte Gréco-Romaine 7–19

778 Cignoni P, Callieri M, Corsini M, et al (2008) MeshLab: an Open-Source Mesh Processing
779 Tool. The Eurographics Association

780 Claude J (2013) Log-Shape Ratios, Procrustes Superimposition, Elliptic Fourier Analysis:
781 Three Worked Examples in R. Hystrix Ital J Mammal 24:94–102.
782 https://doi.org/10.4404/hystrix-24.1-6316

783 Collyer ML, Sekora DJ, Adams DC (2015) A method for analysis of phenotypic change for
784 phenotypes described by high-dimensional data. Heredity 115:357

785 Drake AG, Coquerelle M, Kosintsev PA, et al (2017) Three-dimensional geometric
786 morphometric analysis of fossil canid mandibles and skulls. Sci Rep 7:9508.
787 https://doi.org/10.1038/s41598-017-10232-1

788 Drake AG, Klingenberg CP (2010) Large-scale diversification of skull shape in domestic
789 dogs: disparity and modularity. Am Nat 175:289–301. https://doi.org/10.1086/650372

790 Dryden IL, Mardia KV (2016) Statistical Shape Analysis: With Applications in R. John Wiley
791 & Sons

792 Dunand F, Lichtenberg R, Callou C, Willemin FL (2017) El-Deir nécropoles: Les chiens
793 momifiés d'El-Deir. IV. Cybele Editions

794 Dunand F, Lichtenberg R, Charron A (2005) Des animaux et des hommes: une symbiose
795 égyptienne. Monaco, Monaco, France

796 Durisch Gauthier N (2002) Anubis et les territoires cynopolites selon les temples
797 ptolémaïques et romains. University of Geneva

798 Evin A, Bonhomme V, Claude J (2020) Optimizing digitalization effort in morphometrics.
799 Biol Methods Protoc 5:bpaa023. https://doi.org/10.1093/biomethods/bpaa023

800 Evin A, Bouby L, Bonhomme V, et al (2022) Archaeophenomics of ancient domestic plants
801 and animals using geometric morphometrics : a review. Peer Community J 2:.
802 https://doi.org/10.24072/pcjournal.126

803 Evin A, Cucchi T, Cardini A, et al (2013) The long and winding road: identifying pig
804 domestication through molar size and shape. J Archaeol Sci 40:735–743.
805 https://doi.org/10.1016/j.jas.2012.08.005

806 Evin A, Flink LG, Bălăşescu A, et al (2015) Unravelling the complexity of domestication: a
807 case study using morphometrics and ancient DNA analyses of archaeological pigs
808 from Romania. Philos Trans R Soc B Biol Sci. https://doi.org/10.1098/rstb.2013.0616

809 Evin A, Souter T, Hulme-Beaman A, et al (2016) The use of close-range photogrammetry in
810 zooarchaeology: Creating accurate 3D models of wolf crania to study dog

811 domestication. J Archaeol Sci Rep 9:87–93.
812 https://doi.org/10.1016/j.jasrep.2016.06.028

813 Fabre A-C, Cornette R, Huyghe K, et al (2014) Linear versus geometric morphometric
814 approaches for the analysis of head shape dimorphism in lizards. J Morphol 275:1016–
815 1026. https://doi.org/10.1002/jmor.20278

816 Fau M, Cornette R, Houssaye A (2016) Photogrammetry for 3D digitizing bones of mounted
817 skeletons: Potential and limits. Comptes Rendus Palevol 15:968–977.
818 https://doi.org/10.1016/j.crpv.2016.08.003

819 Foote M (1997) The Evolution of Morphological Diversity. Annu Rev Ecol Syst 28:129–152

820 Forbes-Harper JL, Crawford HM, Dundas SJ, et al (2017) Diet and bite force in red foxes:
821 ontogenetic and sex differences in an invasive carnivore. J Zool 303:54–63.
822 https://doi.org/10.1111/jzo.12463

823 Galov A, Fabbri E, Caniglia R, et al (2015) First evidence of hybridization between golden
824 jackal (*Canis aureus*) and domestic dog (*Canis familiaris*) as revealed by genetic
825 markers. R Soc Open Sci 2:150450. https://doi.org/10.1098/rsos.150450

826 Goodall C (1991) Procrustes methods in the statistical analysis of shape. J R Stat Soc Ser B
827 Methodol 53:285–321

828 Gopalakrishnan S, Sinding M-HS, Ramos-Madrigal J, et al (2018) Interspecific Gene Flow
829 Shaped the Evolution of the Genus Canis. Curr Biol 28:3441-3449.e5.
830 https://doi.org/10.1016/j.cub.2018.08.041

831 Hartley ML (2017) Paws in the sand: the emergence and development of the use of canids in
832 the funerary practice of the ancient Egyptians (ca. 5000 BC–395 AD). Macquarie
833 University, Department of Ancient History

834 Ikram S (2013) Man's Best Friend For Eternity: Dog And Human burials In Ancient Egypt.
835 Anthropozoologica 48:299–307. https://doi.org/10.5252/az2013n2a8

836 Jeanjean M, Haruda A, Salvagno L, et al (2022) Sorting the flock: Quantitative identification
837 of sheep and goat from isolated third lower molars and mandibles through geometric
838 morphometrics. J Archaeol Sci 141:105580. https://doi.org/10.1016/j.jas.2022.105580

839 Khosravi R, Rezaei HR, Kaboli M (2013) Detecting hybridization between Iranian wild wolf
840 (Canis lupus pallipes) and free-ranging domestic dog (Canis familiaris) by analysis of
841 microsatellite markers. Zoolog Sci 30:27–34. https://doi.org/10.2108/zsj.30.27

842 Kitagawa C (2016) The tomb of the dogs at Asyut: faunal remains and other selected objects.
843 Harrassowitz Verlag, Wiesbaden

844 Klingenberg CP (2016) Size, shape, and form: concepts of allometry in geometric
845 morphometrics. Dev Genes Evol 226:113–137. https://doi.org/10.1007/s00427-016-
846 0539-2

847 Klingenberg CP, Monteiro LR (2005) Distances and Directions in Multidimensional Shape
848 Spaces: Implications for Morphometric Applications. Syst Biol 54:678–688.
849 https://doi.org/10.1080/10635150590947258

850 Koepfli K-P, Pollinger J, Godinho R, et al (2015) Genome-wide Evidence Reveals that
851 African and Eurasian Golden Jackals Are Distinct Species. Curr Biol 25:2158–2165.
852 https://doi.org/10.1016/j.cub.2015.06.060

853 Kovarovic K, Aiello LC, Cardini A, Lockwood CA (2011) Discriminant function analyses in
854 archaeology: are classification rates too good to be true? J Archaeol Sci 38:3006–
855 3018. https://doi.org/10.1016/j.jas.2011.06.028

856 Lima RD, Sykora T, Meyer MD, et al (2018) On Combining Epigraphy, TLS,
857 Photogrammetry, and Interactive Media for Heritage Documentation: The Case Study
858 of Djehutihotep's Tomb in Dayr al-Barsha. Eurographics Workshop Graph Cult Herit
859 5 pages. https://doi.org/10.2312/GCH.20181367

860 Lortet LCE, Gaillard C (1903) La faune momifiée de l'Ancienne Egypte. Publ Mus Conflu 1–
861 205

862 Lortet LCE, Gaillard C (1907) La faune momifiée de l'ancienne Egypte (deuxième série).
863 Publ Mus Conflu 1–130

864 Machado FA, Teta P (2020) Morphometric analysis of skull shape reveals unprecedented
865 diversity of African Canidae. J Mammal 101:349–360.
866 https://doi.org/10.1093/jmammal/gyz214

867 Mallil K, Justy F, Rueness EK, et al (2020) Population genetics of the African wolf (Canis
868 lupaster) across its range: first evidence of hybridization with domestic dogs in Africa.
869 Mamm Biol 100:645–658. https://doi.org/10.1007/s42991-020-00059-1

870 Mitteroecker P, Bookstein F (2011) Linear Discrimination, Ordination, and the Visualization
871 of Selection Gradients in Modern Morphometrics. Evol Biol 38:100–114.
872 https://doi.org/10.1007/s11692-011-9109-8

873 Mitteroecker P, Gunz P (2009) Advances in Geometric Morphometrics. Evol Biol 36:235–
874 247. https://doi.org/10.1007/s11692-009-9055-x

875 Mosimann JE (1970) Size allometry: size and shape variables with characterizations of the
876 lognormal and generalized gamma distributions. J Am Stat Assoc 65:930–945.
877 https://doi.org/10.1080/01621459.1970.10481136

878 Murnane W, Ikram S, Dodson A (2000) The Mummy in Ancient Egypt: Equipping the Dead
879 for Eternity. J Am Orient Soc 120:97. https://doi.org/10.2307/604889

880 Osborn DJ, Osbornová J (1998) The mammals of ancient Egypt. Aris & Phillips Warminster

881 Parés-Casanova PM, Salamanca-Carreño A, Crosby-Granados RA, Bentez-Molano J (2020)
882 A Comparison of Traditional and Geometric Morphometric Techniques for the Study
883 of Basicranial Morphology in Horses: A Case Study of the Araucanian Horse from
884 Colombia. Anim Open Access J MDPI 10:E118. https://doi.org/10.3390/ani10010118

885 Porcier SM, Berruyer C, Pasquali S, et al (2019) Wild crocodiles hunted to make mummies in
886 Roman Egypt: Evidence from synchrotron imaging. J Archaeol Sci 110:105009.
887 https://doi.org/10.1016/j.jas.2019.105009

888 Prada L, Wordsworth PD (2018) Evolving Epigraphic Standards in the Field: Documenting
889 Late Period and Graeco-Roman Egyptian Graffiti through Photogrammetry at Elkab.
890 Brill

891 R Core Team (2021) R: A language and environment for statistical computing. R Foundation
892 for Statistical Computing, Vienna, Austria.

893 Richardin P, Porcier S, Ikram S, et al (2017) Cats, Crocodiles, Cattle, and More: Initial Steps
894 Toward Establishing a Chronology of Ancient Egyptian Animal Mummies.
895 Radiocarbon 59:595–607. https://doi.org/10.1017/RDC.2016.102

896 Roberts T, McGreevy P, Valenzuela M (2010) Human induced rotation and reorganization of
897 the brain of domestic dogs. PLOS ONE 5:e11946.
898 https://doi.org/10.1371/journal.pone.0011946

899 Rohlf F, Slice D (1990) Extensions of the Procrustes Method for the Optimal Superimposition
900 of Landmarks. Syst Zool 39:40–59. https://doi.org/10.2307/2992207

901 Rueness EK, Asmyhr MG, Sillero-Zubiri C, et al (2011) The Cryptic African Wolf: Canis
902 aureus lupaster Is Not a Golden Jackal and Is Not Endemic to Egypt. PLOS ONE
903 6:e16385. https://doi.org/10.1371/journal.pone.0016385

904 Saleh M, Younes M, Basuony A, et al (2018) Distribution and phylogeography of Blanford's
905 Fox, Vulpes cana (Carnivora: Canidae), in Africa and the Middle East. Zool Middle
906 East 64:9–26. https://doi.org/10.1080/09397140.2017.1419454

907 Schenkel W (2007) Color terms in ancient Egyptian and Coptic. In: MacLaury RE, Paramei
908 GV, Dedrick D (eds) Anthropology of Color. John Benjamins Publishing Company,
909 Amsterdam, pp 211–228

910 Schenkel W (1963) Die Farben in ägyptischer Kunst und Sprache. Z Für Ägyptische Sprache
911 Altertumskunde 88:131–147. https://doi.org/10.1524/zaes.1963.88.jg.131

912 Schlager S (2017) Chapter 9 - Morpho and Rvcg – Shape Analysis in R: R-Packages for
913 Geometric Morphometrics, Shape Analysis and Surface Manipulations. In: Zheng G,
914 Li S, Székely G (eds) Statistical Shape and Deformation Analysis. Academic Press, pp
915 217–256

916 Thiringer M (2020) An Egyptian's Best Friend? An Analysis and Discussion of the Depiction
917 of the Domestic Dog in Ancient Egypt. Electron Theses Diss

918 Vasilyev S, Vasilyeva O, Galeev R, et al (2019) 3D RECONSTRUCTION OF THE
919 ANCIENT EGYPTIAN MUMMY SKELETON FROM THE PUSHKIN STATE
920 MUSEUM OF FINE ARTS (I,1 1240). ISPRS - Int Arch Photogramm Remote Sens
921 Spat Inf Sci XLII-2/W12:225–229. https://doi.org/10.5194/isprs-archives-XLII-2-
922 W12-225-2019

923 Viranta S, Atickem A, Werdelin L, Stenseth NChr (2017) Rediscovering a forgotten canid
924 species. BMC Zool 2:6. https://doi.org/10.1186/s40850-017-0015-0

925 Von den Driesch A (1976) A guide to the measurement of animal bones from archaeological
926 sites: as developed by the Inst. für Palaeoanatomie, Domestikationsforschung u.
927 Geschichte d. Tiermedizin of the Univ. of Munich. Peabody Museum Press

928 Wiley DF, Amenta N, Alcantara DA, et al (2005) Evolutionary morphing. In: VIS 05. IEEE
929 Visualization, 2005. pp 431–438

930 Wilson D, Reeder D (2005) Mammal Species of The World: A Taxonomic and Geographic
931 Reference

932 Younes MI, Fouad F (2016) Cranial allometry, sexual dimorphism and age structure in
933 sample of the Egyptian wolf canisanthuslupaster. Al-Azhar Bull Sci 27:1–8

934 Yoyotte J, Charvet P, Gompertz S (1997) Strabon. Le voyage en Egypte: un regard romain.
935 NiL Éd.

936 Zelditch ML, Swiderski DL, Sheets HD (2012) Geometric Morphometrics for Biologists: A
937 Primer. Academic Press

938